Quantum Semiclass. Opt. **10** (1998) 823–837. Printed in the UK PII: S1355-5111(98)96001-8

Interaction of spatial photorefractive solitons

Wiesław Królikowski†, Cornelia Denz‡, Andreas Stepken‡, Mark Saffman§ and Barry Luther-Davies†

† Australian Photonics Cooperative Research Centre, Laser Physics Centre, Australian National University, Canberra, ACT 0200, Australia

‡ Institute of Applied Physics, Technische Hochschule Darmstadt, Hochschulstraße, 64289 Darmstadt, Germany

§ Optics and Fluid Dynamics Department, Risø National Laboratory, Postbox 49, DK-4000 Roskilde, Denmark

Received 3 July 1998

Abstract. We present a review of our recent theoretical and experimental results on the interaction of two-dimensional solitary beams in photorefractive SBN crystals. We show that the collision of coherent solitons may result in energy exchange, fusion of the interacting solitons, the birth of a new solitary beam or the complete annihilation of some of them, depending on the relative phase of the interacting beams. In the case of mutually incoherent solitons, we show that the photorefractive nonlinearity leads to an anomalous interaction between solitons. Theoretical and experimental results reveal that a soliton pair may experience both attractive and repulsive forces, depending on their mutual separation. We also show that strong attraction leads to periodic collision or helical motion of solitons depending on initial conditions.

1. Introduction

Photorefractive crystals biased with a DC electric field have been shown to support the formation and propagation of the so-called screening spatial solitons at very moderate laser powers. This is in contrast to experimental realizations of spatial solitons in a traditional Kerr-type material with electronic-type nonlinearity which requires rather high light intensities.

As an optical beam propagates in a photorefractive crystal, the distribution of photoexcited charges induces a space-charge electric field which screens out the externally applied DC field. The effective spatially varying electric field modulates the refractive index of the medium in such a way that the beam becomes self-trapped by a locally increased refractive index and may propagate as a spatial soliton [1–6]. The ease of their formation and manipulation using very low laser power (μW) as well as their stability and robustness makes these screening solitons very attractive for practical applications. Because of their accessibility, screening solitons have also become a very useful tool in experimental verification of many theoretical predictions of general soliton theory, in particular, soliton collision.

Spatial solitons are ideally suited for application in all-optical beam switching and manipulation. This concept is based on the ability to implement logic operations by allowing solitons to collide in a nonlinear medium [8, 9] as well as the possibility of soliton-induced waveguides being used to guide and switch additional beams [10, 11]. Efficient implementation of this idea requires a detailed understanding of the nature of the soliton

1355-5111/98/060823+15$19.50

interaction. In this work we present a review of our recent experimental and theoretical studies on interaction and collision of photorefractive screening solitons.

This paper is organized as follows. In section 2 we present a theoretical model of the formation and propagation of screening solitons in photorefractive media. Section 3 describes the basic experimental configuration used in our studies. Section 4 is devoted to coherent interaction of screening solitons and describes effects such as energy exchange between solitons, soliton birth and annihilation. Next, in section 5 we discuss the interaction of incoherent solitons. We demonstrate soliton attraction, spiralling as well as a unique phenomenon of repulsion of incoherent optical solitons which is due to the anisotropic nature of the photorefractive nonlinearity. Finally, section 6 concludes the paper.

2. Theoretical model

The two-dimensional analysis of the formation, stability and the nonlinear evolution of the (2 + 1)D soliton-type structures in photorefractive media is crucial to a complete understanding of collisional properties of solitons. This is because of the special features of the photorefractive nonlinearity. A photorefractive material responds to the presence of an optical field $B(\vec{r})$ by a nonlinear change in the refrative index Δn that is both an anisotropic and nonlocal function of the light intensity. The anisotropy does not allow radially symmetric soliton solutions thereby requiring explicit treatment of both transverse coordinates. The nonlocality is another feature of the photorefractive response that makes it significantly different from typical nonlinear optical media where the nonlinear refractive index change is a local function of the light intensity. This local response, in the simplest case of an ideal Kerr-type medium $\Delta n \propto |B|^2$, results in the canonical nonlinear Schrödinger equation for the amplitude of light propagating in the medium. A more realistic model results in the appearance of higher-order nonlinearities which are an indication of the saturable (but still local) character of the nonlinearity [12]. In contrast, in photorefractive media the change in the refractive index is proportional to the amplitude of the static electric field induced by the optical beam. Finding the material response therefore requires solving an elliptical-type equation for the electrostatic potential with a source term due to light-induced generation of mobile carriers. The corresponding elliptic boundary-value problem has to be treated globally in the whole volume of the nonlinear medium.

When the spatial scale of the optical beam with amplitude $B(\vec{r})$ is larger than the photorefractive Debye length and the diffusion field may be neglected, the steady state propagation of this beam along the z-axis of the photorefractive crystal with an externally applied electric field along the x-axis is described by the following set of equations [13]:

$$\left[\frac{\partial}{\partial z} - \frac{\mathrm{i}}{2}\nabla^2\right] B(\vec{r}) = \mathrm{i}\frac{\partial \varphi}{\partial x} B(\vec{r}) \tag{1a}$$

$$\nabla^2 \varphi + \ln(1 + |B|^2) \cdot \nabla \varphi = \frac{\partial}{\partial x} \ln(1 + |B|^2). \tag{1b}$$

Here, $\nabla = \hat{x}(\partial/\partial x) + \hat{y}(\partial/\partial y)$ and φ is the dimensionless electrostatic potential induced by the beam with the boundary conditions $\nabla\varphi(\vec{r} \to \infty) \to 0$. The dimensionless coordinates (x, y, z) are related to the physical coordinates (x', y', z') by the expressions $z = \alpha z'$ and $(x, y) = \sqrt{k\alpha}(x', y')$, where $\alpha = \frac{1}{2}kn^2 r_{\mathrm{eff}} E_{\mathrm{ext}}$. Here, k is the wavenumber of light in the medium, n is the refractive index, r_{eff} is the effective element of the electro-optic tensor and E_{ext} is the amplitude of the external field directed along the x-axis far from the beam. The normalized intensity $I = |B(\vec{r})|^2$ is measured in units of the saturation intensity I_{sat}. The

strong anisotropy of the photorefractive nonlinearity is reflected in the elliptical intensity profile of the solution of equation (1*b*) [15]. Complete derivations of the solutions and their discussion can be found in [15].

3. Experimental configuration

All soliton interaction scenarios are investigated experimentally in a configuration shown schematically in figure 1. Three different photorefractive strontium barium niobate crystals were used. They measured $10 \times 6 \times 5, 13 \times 6 \times 6$ and $5 \times 5 \times 5$ mm^3 ($\hat{a} \times \hat{b} \times \hat{c}$), respectively. The first two samples were doped with cerium (0.002% by weight), while the third one was nominally pure. The crystal was biased with a high-voltage DC field of about 2–3 kV applied along its polar *c*-axis. Two circular beams derived from a frequency-doubled Nd:YAG or an argon-ion laser ($\lambda = 532$ or 514.5 nm, respectively) were directed by a system of mirrors and beamsplitters on to the entrance face of the crystal. At this location, the beams had Gaussian diameters of 15 μm, and were polarized along the x-axis (which coincides with the polar axis of the crystal) to make use of the r_{33} electro-optic coefficient, which had a measured value of 180 pm V^{-1}.

The photorefractive nonlinearity has a saturable character. Thus, the parameters of screening solitons are determined by the degree of saturation which is defined as the ratio of the soliton peak intensity to the intensity of the background illumination. The degree of saturation determines not only the steady state parameters of the screening solitons, but more importantly the rate of convergence of input beams to a soliton solution. For moderate saturation ($I \approx 1$) this convergence is fast enough for the solitons to be observed under typical experimental conditions. On the other hand, for strong saturation the convergence is much weaker so an initial Gaussian beam exhibits long transients before evolving into a soliton [13, 15]. To control the degree of saturation, we illuminated the crystal either by an auxiliary laser beam co-propagating incoherently with the signal beams or a wide beam derived from a white light source.

In all our experiments the power of each input beam did not exceed a few microwatts and the power of the background illumination was set to such a level that the degree of saturation was approximately equal to 2 for all beams. We checked that with these

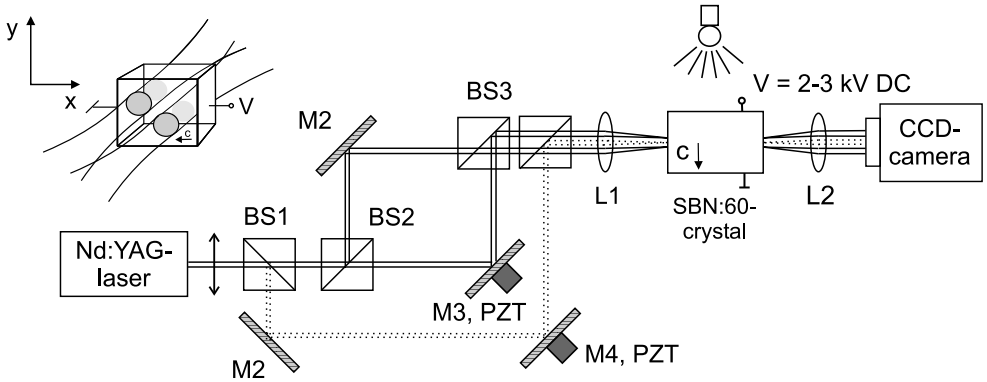

Figure 1. Schematic configuration of soliton interaction. BS, beamsplitters; M, mirrors; L, lenses; PZT, piezoelectric transducer; V, voltage.

parameters all beams would always form elliptically shaped solitons ($\approx 10\,\mu$m wide along the x-axis), when propagating individually in the crystal.

The process of soliton formation was always accompanied by slight self-bending of the soliton's trajectory (several to several tens of μm, depending on the propagation distance). The self-bending results from a nonlocal contribution to the nonlinear refractive index change [4, 16, 17] and increases with decreasing spatial scale of the beam.

One of the input beams was reflected from a mirror mounted on a piezo-electric transducer. By driving this transducer with a DC signal the relative phase of two input beams could be controlled, thus allowing for coherent interaction. On the other hand, using an AC signal of several kHz made the beams effectively incoherent because of the slow response of the photorefractive medium, hence allowing for incoherent interaction. The relative angle of the interacting beams could be adjusted precisely by the external mirrors. In most experiments it did not exceed 1°.

Coherent interaction of solitons propagating in the horizontal plane is always strongly affected by a direct two-wave mixing process that involves phase-independent energy exchange owing to diffraction on the self-induced refractive index grating. To suppress this effect, the incident beams propagated in the vertical plane, perpendicular to the crystal's c-axis. In this way, wave mixing processes can be eliminated and pure soliton–soliton interaction can be observed. The input and output light intensity distributions were recorded with a CCD camera and stored in a computer.

4. Coherent soliton interaction

The nature of the forces exerted by mutually coherent interacting solitons has been discussed in the literature for both temporal [18, 19] as well as spatial solitons [20, 21]. It is well known from the classical investigations of Zakharov and Shabat [22] that solitons governed by integrable models, such as one-dimensional spatial solitons in cubic nonlinear (Kerr) media, behave as particle-like objects. They remain unperturbed when they collide, completely preserving their identities and form. However, the collision of solitons propagating in non-Kerr materials may be drastically different. Nonintegrable models, such as those describing saturable nonlinear media, lead to inelastic collisions, as reflected in the emission of radiation as well as a strong dependence of the outcome of the collision on the relative phase of the solitons [23–25]. In particular, it has been predicted that solitons can annihilate each other, fuse or give birth to new solitons when colliding in nonlinear materials exhibiting a saturation of the nonlinearity. This kind of behaviour is rather generic, being independent of the particular mathematical models for the specific nonlinear medium [25]. Consequently, fusion of solitons was already observed in incoherent soliton collisions in photorefractive crystals [26] as well as during interaction in atomic vapours [27].

It is also well known that in the case of homogeneous self-focusing media the interaction force depends on the relative phase of the solitons. When two solitons are in phase the total light intensity in the area between the beams increases. This, in turn, results in a local increase of the refractive index which effectively attracts both beams. Exactly the opposite situation arises when the solitons are out of phase. Then, the light intensity drops in the interaction region and so the refractive index also drops. This results in the beams moving away from each other, which indicates a repulsive force. Phase-sensitive interaction of spatial solitons has been demonstrated in experiments with various nonlinear media including liquids [28], glass waveguides [29] and photorefractive crystals [30–32].

In our contribution we will describe phase-controlled energy exchange, birth and annihilation of screening photorefractive solitons.

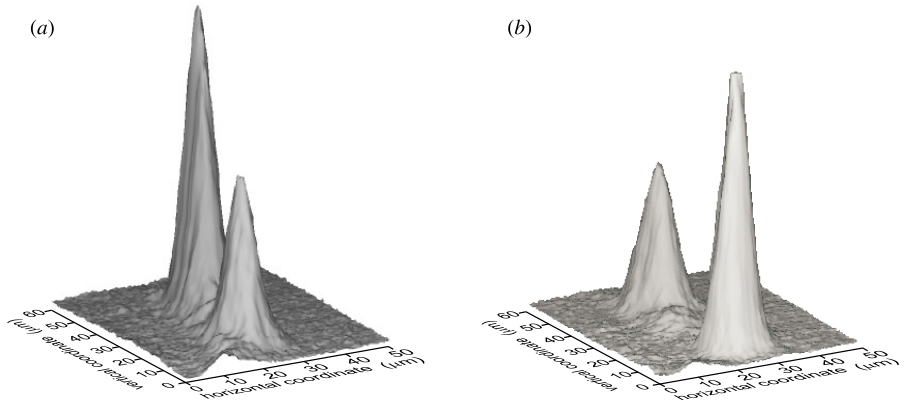

Figure 2. Phase-dependent energy exchange between colliding solitons, intersecting at an angle less than 1°. (*a*) Relative phase close to 90°; (*b*) relative phase close to −90°.

4.1. Energy exchange during collision

Our experiments show that collisions occurring at a large angle are basically elastic—solitons are unaffected by the interaction. The situation is different for small interaction angles (<1°). Then the outcome of the collision depends strongly on the relative phase of the solitons which is a signature of the inelasticity of the collision. In particular, in-phase solitons tend to collapse into a single beam, while out-of-phase solitons clearly repel. For intermediate values of the relative phase the soliton interaction leads to energy exchange. After the collision one soliton would carry more power than the other. This effect is analogous to that found earlier in collisions of solitons described by a perturbed nonlinear Schrödinger equation [19, 33]. In a manner similar to that described in those works, we could also invert the direction of the energy transfer by varying the relative phase of the beams. We illustrate this process in figure 2. The pictures show output intensity profiles of both beams. In this case, both intersect at an angle of about 0.6°. The relative phase is either close to 90° (figure 2(*a*)) or −90° (figure 2(*b*)).

4.2. Soliton birth

It has been predicted that small-angle coherent collisions of two solitons in a saturable medium may give rise to the formation of additional solitons [23, 25]. To observe this so-called 'soliton birth', we set the interaction angle to be about 0.8°. The relative phases between the two beams were chosen in such a way that without an applied field we could clearly observe three distinct interference fringes at the exit face of the crystal. Then, after the electric field was applied, these fringes evolved into three clearly defined solitary beams, as shown in figure 3. Notice that the newly formed central soliton does not propagate in the same plane as the other two. This is due to the higher rate of self-bending experienced by this beam.

4.3. Soliton annihilation

If a soliton birth can be realized by proper adjustment of the phases of two solitons, the reverse effect should also be possible—the annihilation of a soliton due to mutual interaction

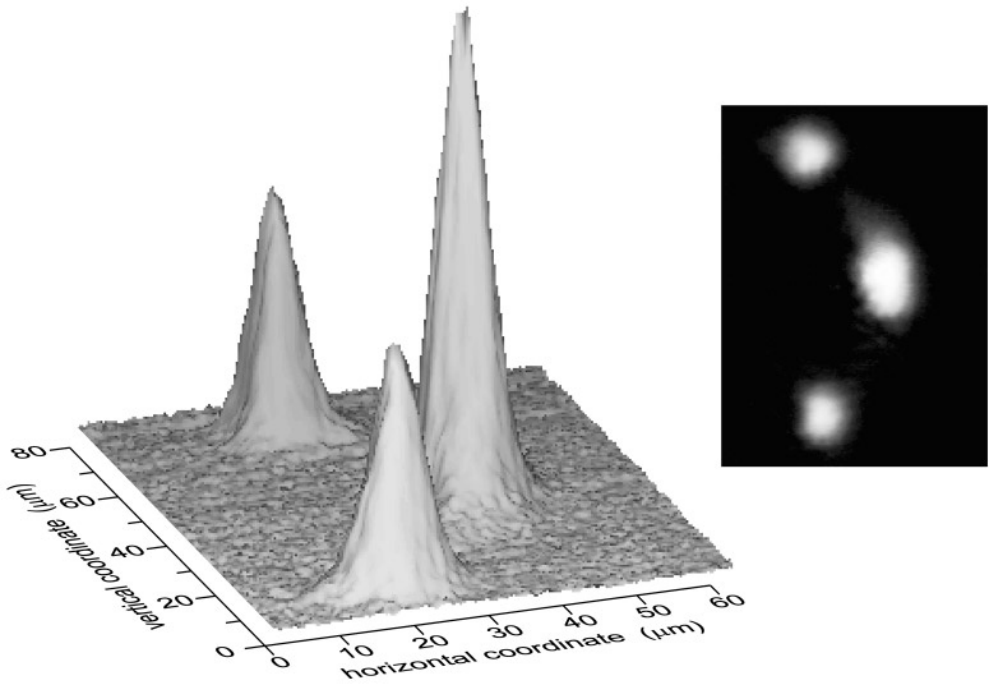

Figure 3. Birth of a new soliton upon collision in a vertical interaction geometry, perpendicular to the direction of the applied electric field. The new central beam experiences a higher rate of self-bending and therefore does not propagate in the same plane as the other two.

during collision. Soliton annihilation was predicted theoretically some time ago [25], but has not been observed so far. To investigate this effect the experimental set-up was slightly modified in order to introduce three beams into the crystal. They all propagated in the vertical plane and were aligned in such a way that they would intersect approximately in the common region of the crystal. The power of the central beam (C) was 1.7 μW, while both side beams (A) and (B) were approximately 4 times weaker. Beams A and B were always in phase, while the phase of the beam C measured at the output face of the crystal was used as a control parameter. The results of the three-soliton collision are presented in figure 4, which shows the light intensity of the outgoing beams after interaction as seen on the exit face of the crystal. In the example depicted in figure 4(a) the relative phase between A, B and C is close to $\pi/2$. The very bright spot corresponds to the central soliton (C), while two faint ones correspond to both side beams (A and B). Careful examination of this picture reveals that the power of the central beam increases at the expense of A and B. The latter two still propagate as very well defined solitary beams although they are weaker. The situation changes dramatically when the relative phase of beam C is adjusted to $-\pi/2$ (figure 4(b)). Clearly, now the central beam virtually disappears, while two new strong symmetrically located solitons appear. Note that the relative locations of these new beams differ from those in figure 4(a).

The underlying process responsible for annihilation of the central beam is the already discussed phase-dependent energy exchange between colliding solitons. In the first instance shown in figure 4(a) the relative phase of the beams is chosen such that if both soliton A and soliton B supply energy to C, when the phase of the beam C is changed to $-\pi/2$

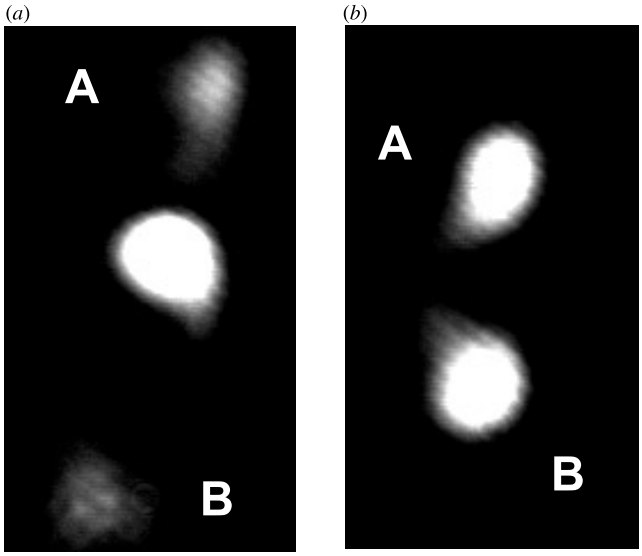

Figure 4. Three-soliton interaction, $P_A = P_B = 0.4\ \mu W$, $P_C = 1.7\ \mu W$: (*a*) relative phase between A and C $\approx \pi/2$; (*b*) relative phase between A and C $\approx -\pi/2$.

(figure 4(*b*)) the power flows outwards to the side beams. Consequently, both solitons A and B are amplified at the expense of C, which results in effective annihilation of the latter.

5. Interaction of incoherent solitons

In typical isotropic self-focusing media mutually incoherent solitons always attract each other. This is because the total light intensity always increases in the region where the beams overlap. This leads to an increase of the refractive index and subsequent attraction of the solitons. Several recent works have studied incoherent soliton interactions in photorefractive media where the physics is quite similar to that pertaining in saturable Kerr-type media [36]. Here, we will show that it is possible to achieve both attractive *and* repulsive forces between mutually incoherent solitons. This anomalous situation occurs in photorefractive media where the particular anisotropic and nonlocal structure of the nonlinearity results in both attraction and repulsion of parallel beams depending on their relative spatial separation. We will present a numerical simulation of this behaviour and show experimental results on soliton attraction, repulsion and mutual rotation of initially parallel and skewed beams.

5.1. Anisotropic nonlinear response

When two incoherent beams propagate through the photorefractive nonlinear medium, the optical field can be represented by two amplitudes

$$B(\vec{r}, t) = \left[B_1(\vec{r}, t) + B_2(\vec{r}, t)\exp(-\mathrm{i}\Omega t)\right]\exp[\mathrm{i}(kz - \omega t)] \tag{2}$$

separated by a frequency shift Ω such that $\Omega\tau \gg 1$, where τ is the characteristic response time of the nonlinearity. Their steady state propagation along the z-axis is described by an obvious generalization of the model described in section 2,

$$\left[\frac{\partial}{\partial z} - \frac{\mathrm{i}}{2}\nabla^2\right] B_1(\vec{r}) = \mathrm{i}\frac{\partial\varphi}{\partial x} B_1(\vec{r}) \tag{3a}$$

$$\left[\frac{\partial}{\partial z} - \frac{\mathrm{i}}{2}\nabla^2\right] B_2(\vec{r}) = \mathrm{i}\frac{\partial\varphi}{\partial x} B_2(\vec{r}) \tag{3b}$$

$$\nabla^2\varphi + \nabla\varphi\cdot\nabla\ln(1+|B_1|^2+|B_2|^2) = \frac{\partial}{\partial x}\ln(1+|B_1|^2+|B_2|^2). \tag{3c}$$

Here again, the normalized intensity $I = |B_1|^2 + |B_2|^2$ is measured in units of saturation intensity I_{sat}.

Numerical solutions of equation (3*c*) for $B_{1,2} = \sqrt{2.3}\exp[-[(x \pm d/2)^2 - y^2]/4]$, for several values of the separation d along the direction of the applied field (x-axis) are shown in figure 5. In this figure, the nonlinear refractive index $\Delta n \sim \partial\varphi/\partial x$ has been visualized. For small values of the separation (figure 5(*a*)) the structure of the nonlinear refractive index is similar to that due to a single beam [6, 14]. The peak centred at $x = y = 0$ leads to self-focusing and attraction of the beams. The essentially anisotropic nature of the nonlinearity is seen in the tails of the refractive index distribution. Along the y-axis, where the refractive index decays monotonically to zero, the structure is analogous to that seen for a Kerr-type nonlinearity ($\Delta n \sim I$). Therefore, one may expect that beams separated along the y-axis will attract each other, as is the case for typical solitons in Kerr-type media.

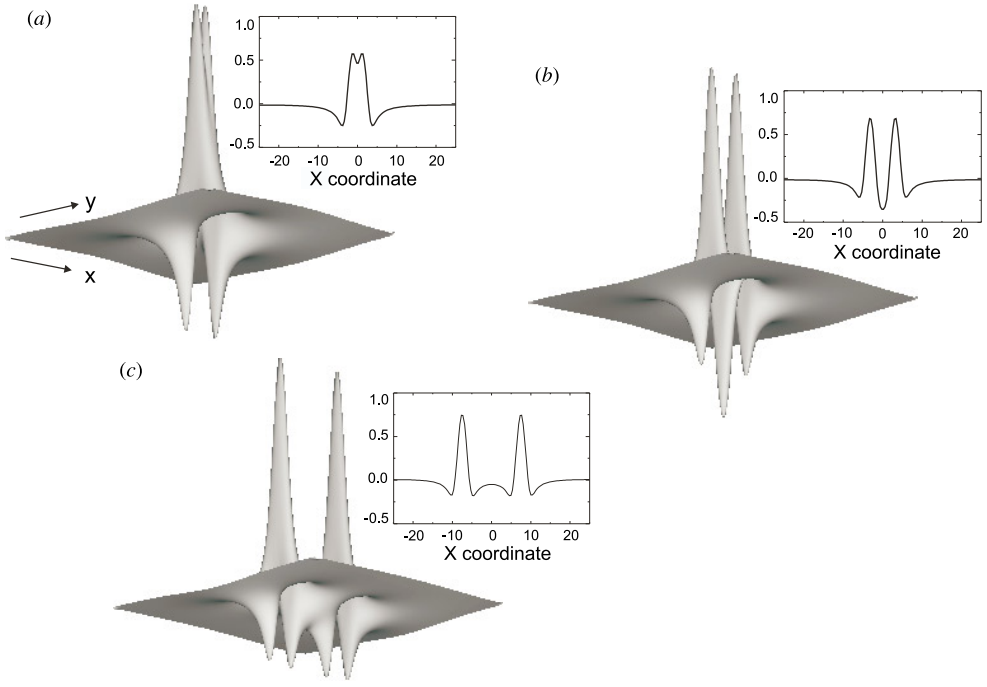

Figure 5. Nonlinear refractive index for beam separation d equal to 3 (*a*), 7 (*b*) and 15 (*c*). The computational window was a square with widths $L_x = L_y = 50$. The inset plots show the variation of the refractive index in units of 10^{-4} along the x coordinate for $y = 0$..

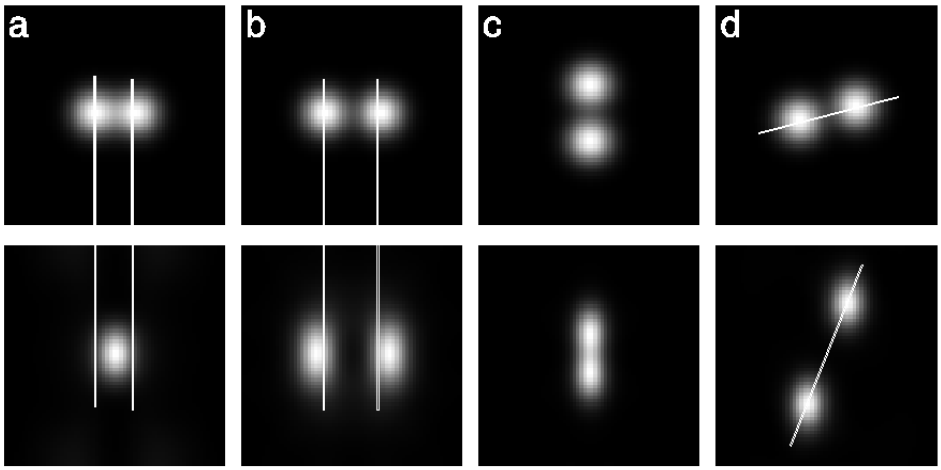

Figure 6. Result of numerical calculations of propagation through a distance $l_z = 38$ for initial separation d_x equal to 3 (a), 7 (b) and 15 (c). In case (d) $d_x = 5$, $d_y = 1.5$. Other parameters are as in figure 5.

Along the x-axis, however, the central peak is surrounded by regions of both positive and negative Δn. Sufficiently far from the centre of the beam the refractive index actually increases with decreasing light intensity, which corresponds to a self-defocusing behaviour. When the separation is increased to $d = 7$ (figure 5(b)) the negative index regions induced by each beam overlap, resulting in an even larger dip in the index between the beams. It is exactly this circumstance that results in the observed repulsion of mutually incoherent beams. For larger values of the separation (figure 5(c)) the regions of negative refractive index are less deep and the beams repel each other weakly.

5.2. Anomalous interaction

The propagation dynamics of two solitons were investigated by numerical integration of equations (3) for initial separations corresponding to those shown in figure 5. The closely spaced input beams (figure 6(a), top row) attract each other strongly, and eventually coalesce into a single beam after propagating over a distance $l_z = 38$ (bottom row). This behaviour is generic for solitons in saturable nonlinear media [23, 24] colliding at a very small angle. An essentially different behaviour can be seen in figure 6(b) where the initial separation is $d_x = 5.3$. The separation between the solitons increases with propagation distance indicating mutual repulsion. Note that also in this case each beam attains an elliptical shape with the diameter ratio $\sim$1.5, characteristic for photorefractive solitons. For the same initial separation, but oriented along the y-axis (figure 6(c)), the beams attract each other. Finally, for initial separation along both x and y, more complex dynamics, including the initial stages of a counterclockwise spiralling motion about the centre of two beams [35] is observed, as shown in figure 6(d).

Experimental results are presented in figure 7 where we show input and output light intensity distributions for two different initial separations of the beams. The first row of figure 7 shows images of both beams at the input face of the crystal. The second row shows the output intensity distribution for noninteracting solitons. These images were obtained by allowing each beam to propagate separately in the crystal and superimposing the resulting

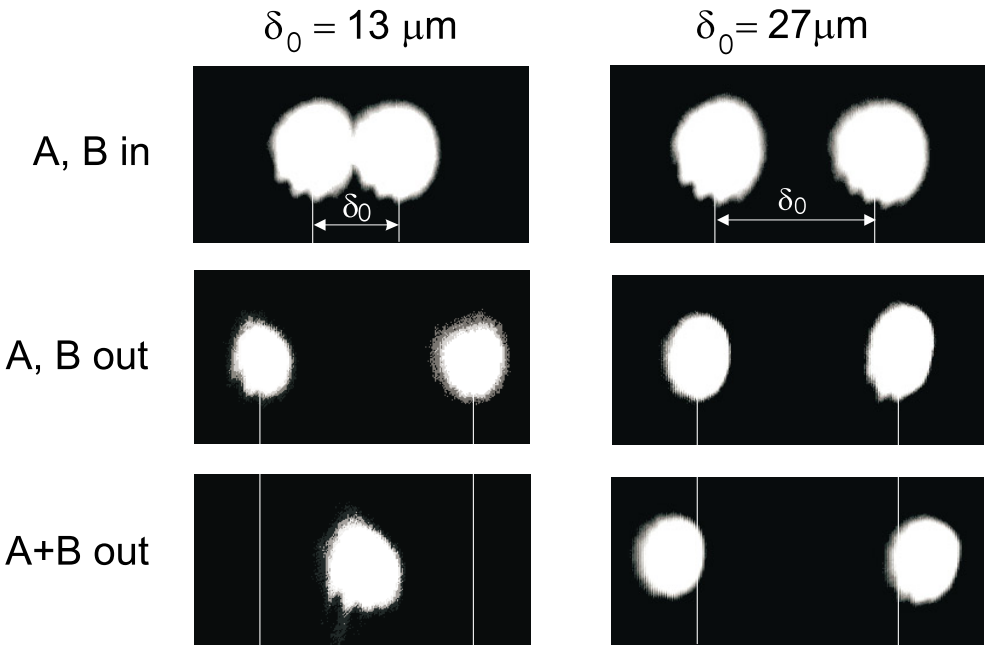

Figure 7. Experimental observation of separation-dependent interaction of incoherent solitons. The x-axis is horizontal. The pictures have been corrected to remove the displacement along x due to self-bending of the solitons.

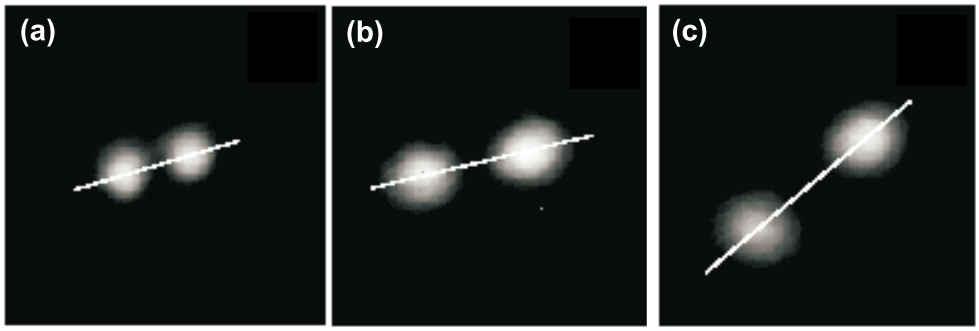

Figure 8. Experimental observation of mutual repulsion and rotation due to anisotropy of nonlinearity. (*a*) Beams at the entrance face of the crystal; (*b*) at the exit face without interaction and (*c*) during spiralling due to the interaction when the external field is operating. Again, the x-axis is horizontal.

images. Finally, the third row contains images of interacting solitons. They were recorded when both beams were present simultaneously in the crystal.

In the case of closely spaced solitons ($d_x \approx 13$ μm, left-hand column in figure 7) the interaction is strongly attractive and the beams fuse emerging from the crystal as a single elliptically shaped solitary beam. This behaviour is essentially the same as that found for strongly overlapping solitons in a saturable Kerr-type nonlinearity. The situation changes dramatically when the initial separation between beams is increased to $d_x \approx 27$ μm

as shown in the right-hand column of figure 7. This time both input beams evolve into separate solitary waves while their separation increases, indicating mutual repulsion. We wish to stress that the interaction of incoherent solitons separated only along y always resulted in their attraction, independent of the magnitude of the initial separation.

As was shown in figure 6(d) more complex behaviour featuring mutual rotation occurs when the input beams are separated along both x and y. We investigated this effect experimentally using the same configuration as above. Mutual rotation was clearly observed and is shown in figure 8. Intensity profiles presented in this figure were obtained with higher saturation than used in the numerical simulations, thus the output beams have not converged to an elliptical shape. The first image (figure 8(a)) shows the intensity distribution of the input beams. They are separated along an axis tilted at $\approx 13^\circ$ with respect to the x-axis. Figures 8(b) and (c) contain output intensity distributions for noninteracting (independent propagation) and interacting solitons, respectively. As is clear from the figure mutual interaction results not only in increased separation between solitons but also in a counterclockwise spiral motion about the centre of the beams, in exactly the same manner as found numerically in figure 6(d). It should be emphasized that the spiralling motion is due to the anisotropy of the potential created by the two beams, and occurs even though they are launched without any tangential velocity.

5.3. Mutual oscillation of incoherent solitons

We have already pointed out that for incoherent photorefractive solitons propagating in the plane perpendicular to the direction of the applied electric field, the nonlinear response of the medium is analogous to that of Kerr-like nonlinearity. For such a nonlinearity, solitons always attract independently of their separation. Moreover, it is well known that attraction of these solitons may result in a nontrivial trajectory character [21]. In particular, beams propagating in the same plane may become bound with their trajectories periodically intersecting. On the other hand, solitons launched skewed to each other into the crystal may exhibit a helical motion. Therefore, photorefractive spatial solitons should also exhibit

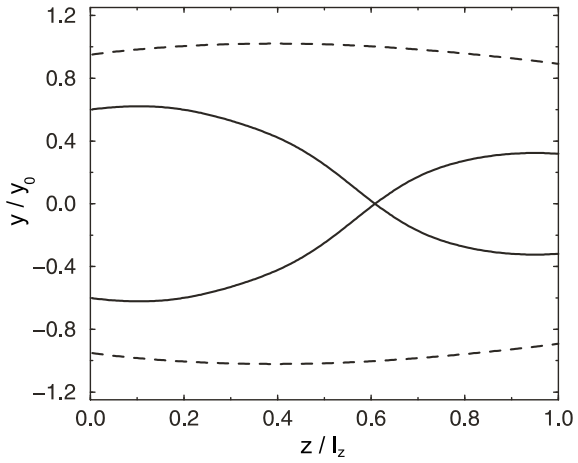

Figure 9. Trajectories of the two incoherent interacting solitons launched initially in the same (vertical) plane. The angular separation of the beams is 1.8 mrad, whereas separation distance and propagation distance are normalized to $y_0 = 14.66$ μm and $l_z = 6.5$ mm, respectively.

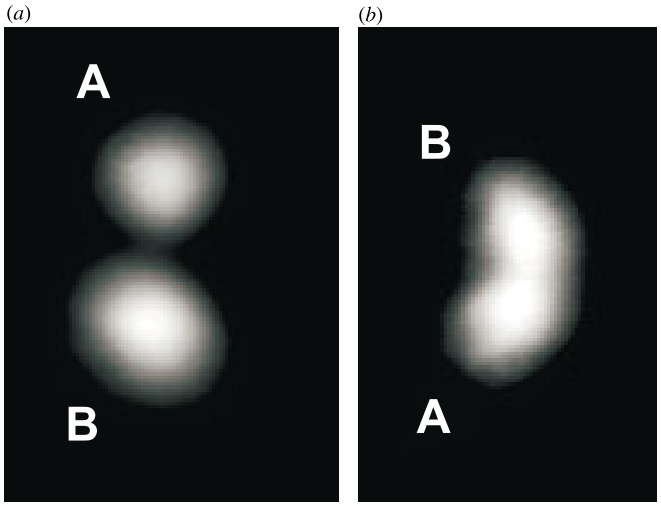

Figure 10. Experimentally observed strong attraction of incoherent solitons propagating in the vertical plane. (*a*) Beams at the entrance face of the crystal; (*b*) beams at the output face. Attraction results in collision and change of the position of both solitons.

a similar behaviour, if arranged properly at the entrance face. To account for an arbitrary beam orientation at the input face, especially for the case of skewed beams, we used a model that allows both beams to propagate with different angles in the photorefractive medium [37]. In figure 9 we show the numerically calculated trajectories of initially parallel solitary beams propagating in the vertical plane. In the first case (broken curve), beams are well separated so mutual attraction is still visible as both trajectories bend towards each other, though rather weak. On the other hand, for smaller separation distances (full curve), the interaction is much stronger and leads to a periodic collision of solitons. However, as each collision is inelastic the amplitude of the mutual oscillation is damped and the solitons would eventually fuse. In figure 10 we demonstrate experimentally this strong attraction of screening solitons. The figure shows the light intensity distribution at the input (figure 10(*a*)) and output (figure 10(*b*)) face of the crystal, respectively. The initial trajectories of both beams were slightly divergent so they would not intersect in the crystal. However, as figure 10(*b*) clearly shows, attraction results in collision and change of position of both solitons.

The same attractive force between closely separated solitons is responsible for mutual spiralling of two solitons propagating initially in different planes (skewed beams). In this case the initial apparent repulsion of beams due to the divergence of their trajectories can be compensated for by mutual attraction. We investigated this effect numerically as well as experimentally. Figure 11 shows the numerically found positions of the solitons during propagation in the crystal. Initially both beams were located along the y-axis with their trajectories inclined at 7 mrad to each other. As the solitons propagate (and interact), their trajectories clearly spiral around each other. For the propagation distance of 6.5 mm the solitons rotate by 180°. In figure 12 we present the experimental evidence of this effect. Figure 12(*a*) shows both beams at the input face of the crystal, while figure 12(*b*) displays the output position of simultaneously propagating solitons. The circles indicate the positions of the solitons when propagating without any interaction. It is clear that attraction of solitons resulted in mutual rotation of their trajectories. In this particular

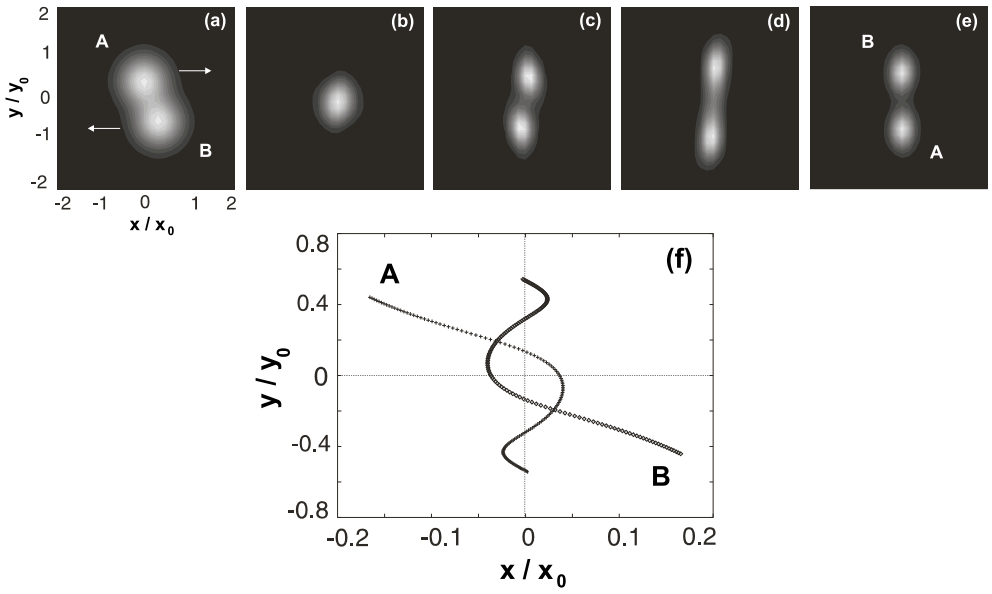

Figure 11. Mutual spiralling of incoherent solitons launched skewed to each other: results of numerical simulations. (*a*) Beams at the entrance face, (*b*) $z = 1.625$ mm, (*c*) 3.25 mm, (*d*) 4.875 mm, (*e*) $z = l_z = 6.5$ mm, (*f*) positions of the two solitons as they propagate through the photorefractive crystal.

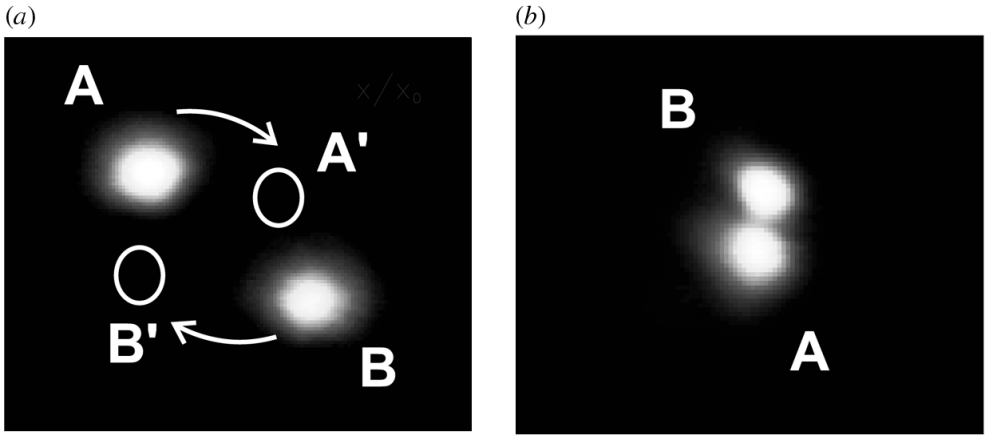

Figure 12. Experimentally observed attraction-induced soliton spiralling: (*a*) input beams, (*b*) interacting solitons. Circles labelled with A′ and B′ represent the output positions of solitons A and B during individual propagation through the crystal (no interaction).

instance the rotation exceeds 180° over 10 mm propagation distance. Interestingly, in a recently published paper on soliton spiralling [35] a stronger rotation of solitons has been reported (almost 540° over a 10 mm distance). Our numerical simulations as well as these experiments indicate that such a high rate of rotation is difficult to achieve because the soliton interaction is always affected by the anomalous interaction described above. This aspect is presently under investigation.

6. Conclusions

In conclusion, we have shown several interaction scenarios of coherent and incoherent soliton beams propagating in a photorefractive medium that allows for applications in beam guiding, switching and optical logic circuitry. We observed collisions in combination with energy exchange, the birth of solitons as well as the phase-controlled fusion and annihilation of solitons. For the case of incoherent interaction, we have shown that spatial solitons in photorefractive media exhibit anomalous interaction properties not seen in isotropic nonlinear media. In particular, while closely overlapping incoherent solitons always attract each other, larger separations may result in repulsive forces depending on the separation and its orientation. This effect is a result of the nonlocal character of the anisotropic self-focusing in photorefractive media which leads to an effective self-defocusing in parts of the outer regions of the optical beam. Close agreement between experiments and the predictions of a three-dimensional model were obtained.

Acknowledgments

WK acknowledges support of the Alexander von Humboldt Stiftung. MS was supported by grants nos 9502764 and 9600852 from the Danish Natural Science Research Council. Contributers from Darmstadt University of Technology acknowledge support from Sonderforschungsbereich 185 'Nonlinear Dynamics' and would like to thank Professor T Tschudi as well as Professor F Kaiser for support and helpful discussions.

References

[1] Iturbe-Castillo M D, Marquez-Aguilar P A, Sanchez-Mondragon J J, Stepanov S and Vysloukh V 1994 *Appl. Phys. Lett.* **64** 408
[2] Segev M, Valley G C, Crosignani B, DiPorto P and Yariv A 1994 *Phys. Rev. Lett.* **73** 3211
[3] Christodoulides D N and Carvalho M I 1995 *J. Opt. Soc. Am.* B **12** 1628
[4] Shih M, Segev M, Valley G C, Salamo G, Crosignani B and DiPorto P 1995 *Electron. Lett.* **31** 826
[5] Sheng Z, Cui Y, Cheng N and Wei Y 1996 *J. Opt. Soc. Am.* B **13** 584
[6] Zozulya A A and Anderson D Z 1995 *Phys. Rev.* A **51** 1520
[7] Hasegawa A and Kodama Y 1995 *Solitons in Optical Communications* (Oxford: Oxford University Press)
[8] Shi T-T and Chi S 1990 *Opt. Lett.* **15** 1123
Snyder A W, Mitchell D J, Poladian L and Ladouceur F 1991 *Opt. Lett.* **16** 21
McLeod R, Wagner K and Blair S 1995 *Phys. Rev.* A **52** 3254
Miller P D and Akhmediev N N 1996 *Phys. Rev.* E **53** 4098
[9] Firth W J and Scroggie A J 1996 *Phys. Rev. Lett.* **76** 1623
Brambilla M, Lugiato L A and Stefani M 1996 *Europhys. Lett.* **34** 109
[10] Luther-Davies B and Yang X 1992 *Opt. Lett.* **17** 498
Luther-Davies B, Yang X and Królikowski W 1993 *Int. J. Nonlin. Opt. Mater.* **2** 339
[11] de la Fuente R, Barthelemy A and Froehly C 1991 *Opt. Lett.* **16** 793
[12] Marburger J H 1975 *Prog. Quantum Electron.* **4** 35
[13] Zozulya A A, Anderson D Z, Mamaev A V and Saffman M 1998 *Phys. Rev.* A **57** 622
[14] Korneev N *et al* 1996 *J. Mod. Opt.* **43** 311
[15] Zozulya A A, Mamaev A V, Saffman M and Anderson D 1996 *Europhys. Lett.* **36** 419
Zozulya A A, Mamaev A V, Saffman M and Anderson D 1996 *Phys. Rev.* A **54** 870
[16] Carvalho M I, Singh S R and Christodoulides D N 1995 *Opt. Commun.* **120** 311
[17] Królikowski W, Akhmediev N, Luther-Davies B and Cronin-Golomb M 1996 *Phys. Rev.* E **54** 5761
[18] Gordon J P 1983 *Opt. Lett.* **11** 596
[19] Kodama Y and Nozaki K 1987 *Opt. Lett.* **12** 1038
Islam M N 1990 *Opt. Lett.* **15** 417

[20] Desem C and Chu P L 1987 *IEEE Proc.* J **134** 145
Taylor J R (ed) 1992 *Optical Solitons—Theory and Experiment* (Cambridge: Cambridge University Press) ch 5
[21] Poladian L, Snyder A W and Mitchell D J 1991 *Opt. Commun.* **85** 59
Mitchell D J, Snyder A W and Poladian L 1996 *Phys. Rev. Lett.* **77** 271
[22] Zakharov V E and Shabat A B 1971 *Zh. Eksp. Teor. Fiz.* **61** 118 (Engl. transl. 1972 *Sov. Phys.–JETP* **34** 62)
[23] Oficjalski J and Białynicki-Birula I 1978 *Acta Phys. Polon.* B **9** 759
[24] Cowan S, Enns R H, Rangnekar S S and Sanghera S 1986 *Can. J. Phys.* **64** 311
Gatz S and Herrmann J 1992 *Opt. Lett.* **17** 484
[25] Snyder A W and Sheppard A P 1993 *Opt. Lett.* **18** 482
[26] Shih M and Segev M 1996 *Opt. Lett.* **21** 1538
[27] Tikhonenko V, Christou J and Luther-Davies B 1996 *Phys. Rev. Lett.* **76** 2698
[28] Reynaud F and Barthelemy A 1990 *Europhys. Lett.* **12** 401
Shalaby M and Barthelemy A 1992 *Opt. Lett.* **16** 1472
[29] Aitchison J S *et al* 1991 *Opt. Lett.* **16** 15
Aitchison J S *et al* 1991 *J. Opt. Soc. Am.* B **8** 1290
[30] García-Quirino G S *et al* 1997 *Opt. Lett.* **22** 154
Meng H, Salamo G, Shih M-F and Segev M 1997 *Opt. Lett.* **22** 448
Mamaev A V, Saffman M and Zozulya A A 1998 *J. Opt. Soc. Am.* B to appear
[31] Królikowski W and Holmstrom S A 1997 *Opt. Lett.* **22** 369
[32] Królikowski W, Luther-Davis B, Denz C and Tschudi T 1998 *Opt. Lett.* **23** 97
[33] Hong B J and Yang C C 1991 *J. Opt. Soc. Am.* B **8** 1114
[34] Królikowski W, Saffman M, Luther-Davies B and Denz C 1998 *Phys. Rev. Lett.* **80** 3240
[35] Shih M, Segev M and Salamo G 1997 *Phys. Rev. Lett.* **78** 2551
[36] Shih M-F *et al* 1996 *Appl. Phys. Lett.* **69** 4151
Shih M-F and Segev M 1996 *Opt. Lett.* **21** 1538
[37] Stepken A, Belic M and Kaiser F 1998 *Asian J. Phys.* to be published